

LETTERS

Equilibrium Shape Diagram for Strained Ge Nanocrystals on Si(001)

R. Stanley Williams,* Gilberto Medeiros-Ribeiro, Theodore I. Kamins, and Douglas A. A. Ohlberg

Hewlett-Packard Laboratories, 3500 Deer Creek Road, MS 26U-12, Palo Alto, California 94304-1392

Received: September 9, 1998

We introduce a chemical-thermodynamic model to explain the formation and annealing behavior of Ge nanocrystalline islands grown on Si(001). Assuming the nanocrystals are essentially large adsorbed molecules, we propose a simple free energy expression for islands of different shapes interacting with each other via the substrate on which they reside. Nanocrystal growth, disappearance, and shape transitions are all consonant with a near-equilibrium system constrained by mass conservation and characterized by interisland repulsions. We construct an equilibrium shape diagram from experimentally determined free energy differences between island shapes and use it to resolve several anomalies that have been noted for the Ge on Si(001) system.

The deposition of Ge onto Si(001), for which the lattice mismatch is +4.2%, has been described as a classic Stranski–Krastanow (SK) process.¹ The SK model supposes that an elastically strained film (or wetting layer) grows pseudomorphically on a lattice-mismatched substrate to a certain thickness, with further deposition leading to the growth of three-dimensional islands on top of the film. Interest in this system increased dramatically after two reports appeared in 1990 in which island formation occurred when 3–8 equivalent monolayers (eq-ML) of Ge were deposited on nominally 500 °C Si(001) substrates.^{2,3} Although these are among the most well-known and often cited studies of SK growth, the results reported by the two groups were remarkably different.

Using transmission electron microscopy (TEM), Eaglesham and Cerullo² observed “dome-shaped” nanocrystals of Ge as large as 140 nm in diameter and 50 nm high that were coherently strained on the substrate. Larger islands contained dislocations that were presumably caused by a plastic relaxation of the islands as they grew beyond a critical size. Even though their experimental growth conditions were nominally the same, Mo et al.³ reported entirely different nanocrystal shapes, primarily rectangular-based “huts” bounded by {105} facets, from their

scanning tunneling microscope (STM) studies. Tomitori et al.⁴ systematically determined a temperature-coverage structure diagram for Ge overlayers on Si(001) from 1 to 8 eq-ML and substrate temperatures of 300, 400, and 500 °C. Their diagram revealed that different island shapes corresponded to certain deposition conditions, but that huts and domes could coexist for Ge deposits of 7 eq-ML and a substrate temperature of 500 °C. At lower temperatures, they did not observe domes for any coverage condition, but at 400 °C and 5–6 eq-ML they observed the coexistence of huts and “macroscopic clusters”, which were also reported by Mo et al. and are essentially the larger dislocated islands of Eaglesham and Cerullo.² Other observations of apparently anomalous behavior in terms of what types of islands form at various equivalent Ge coverages and temperatures below and above 500 °C have been discussed, but no consensus has formed to explain these observations.^{5–8}

We have performed several experiments aimed at understanding the growth and stability of strained nanocrystal islands. These include deposition of Ge overlayers by physical vapor deposition (PVD) in ultrahigh vacuum (UHV) followed by *in situ* analysis with atomic-resolution STM and growth by chemical vapor deposition (CVD) using GeH₄ in an H₂ ambient

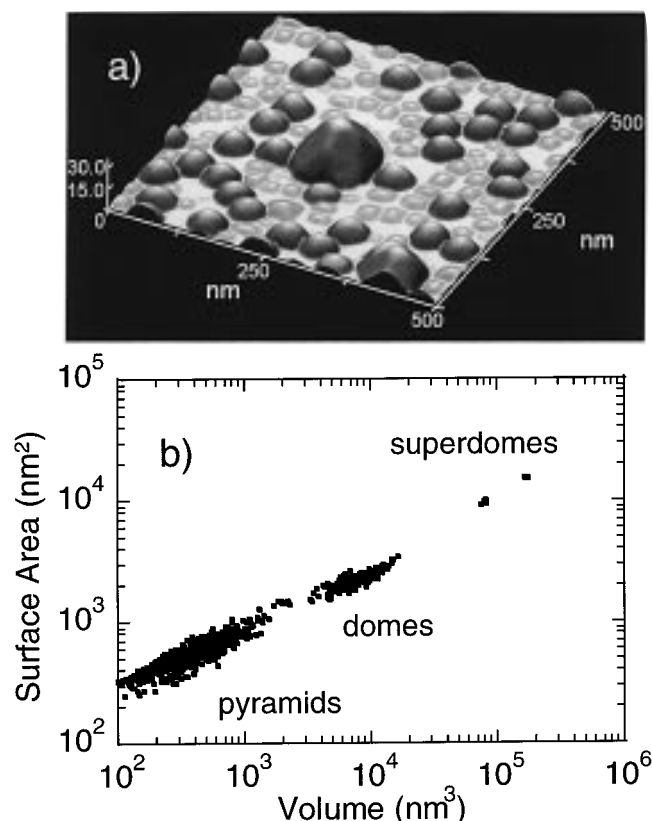


Figure 1. (a) Atomic force microscope topograph of a 13 eq-ML film of Ge deposited onto Si(001) and annealed for 30 min at 550 °C. The gray scale is keyed to the local facet angle with respect to the substrate plane, with darker shades corresponding to steeper angles. Pyramids, domes, and superdomes are readily recognized by both their size and shading. (b) Scatter plot showing the exposed surface area of the islands versus their volumes on a 1 μm^2 area for the same sample as in part a. Each island shape forms a family of points on the graph, allowing the members of each family to be identified for statistical analysis.

followed by ex situ imaging with atomic force microscopy (AFM). When the results of these two types of experiments are compared for approximately the same substrate temperature, growth rate, and amount deposited, the island shapes, sizes, and populations are quite similar (within the limits of the differences in resolution between STM and AFM). The similarities are remarkable given that the background pressures during Ge overlayer growth differed by 11 orders of magnitude and the CVD samples were exposed to air before measurement. The observed behavior of Ge on Si(001) is considerably more complex than that of the idealized SK model.¹ In the temperature range from 550 to 650 °C, experiments from this laboratory^{9–13} have shown that there are three distinct and stable island shapes (see Figure 1a), which we give the descriptive names pyramids, domes, and superdomes, and each can dominate the Ge overlayer under certain conditions. The pyramids are a special case of hut with a square base and four equal-area {105} facets, whereas the domes are actually multifaceted structures characterized primarily by {311} and {518} planes along with small but distinct {105} and (001) facets. The superdomes, which have been given different names by other researchers, are similar in shape to the domes but are much larger, have {111} and other steep facets at the boundary with the substrate, and contain one or more dislocations.^{2,5–8} There are transitions between the different island shapes with changes in Ge coverage and substrate temperature.¹³

An important issue that is not widely recognized is that Ge islands on Si(001) are only metastable with respect to alloying

with the substrate.¹¹ The rate of diffusion of Si into the Ge islands is quite rapid at 650 °C, about 20 times faster than at 600 °C, which corresponds to an activation energy for the alloy formation of approximately 4.2 eV. Alloying must be considered carefully when examining the growth and annealing of Ge islands, since even a small change in the composition of an island can have a dramatic effect upon its strain energy and thus its characteristic volume, which scales as ϵ^{-6} .^{14,15} Thus, the data from experiments that are performed at substrate temperatures ≥ 650 °C is complicated by the fact that the composition of the islands may be changing appreciably during deposition and annealing.

Two different views of the growth and evolution of Ge nanocrystals on Si have emerged that have considerably different consequences for the rational design of strained nanocrystal arrays. One model^{15,16} is that the island sizes and distributions are determined by the kinetic process of Ostwald ripening,¹⁷ whereas the other states that the islands are essentially in thermodynamic (metastable) equilibrium with each other, if not with the substrate.^{10,18,19} If island evolution is primarily a kinetic process, the attempts by researchers to grow stable and uniform nanostructures on surfaces by chemical self-assembly may be impossible, whereas if the islands are at least quasi-equilibrium structures, then they should be stable for some significant amount of time.

The elastically strained Ge islands are compressed at the interface to match the smaller lattice constant of Si, but near the top of the islands the relaxation to the lattice constant of Ge may be nearly complete.²⁰ The Si substrate is somewhat deformed, especially near the edges of an island.^{21–23} These factors make the internal free energy of the islands a nonlinear function of their volume.²³ In the model of Shchukin et al.,¹⁸ the free energy of an island ensemble has a minimum as a function of island volume, which stabilizes the distribution around that island size. The STM measurements of Ge island volumes by Medeiros-Ribeiro et al.¹⁰ were consistent with Boltzmann distributions incorporating the Shchukin et al.¹⁸ free energy expression. This report also showed that the pyramids and domes each had distinct and nonoverlapping size distributions.

An example of the results of a CVD growth and annealing experiment are shown in Figure 1a. A controlled amount of Ge, 13 eq-ML as determined by Rutherford backscattering (RBS), was deposited onto a 550 °C Si(001) substrate and imaged ex situ using AFM.¹² The volume and surface area of 821 islands were measured from the high-resolution AFM topograph of Figure 1a and are presented as a scatter plot in Figure 1b. Both the topograph and scatter plot in Figure 1 show that all three island shapes can coexist with each other, and the size distributions and relative populations of the different island shapes are little changed for this coverage even after 1 h of annealing at 550 °C.¹² In this case, the superdomes are fewest in number density on the surface, but they contain the majority of the material in islands as determined by comparing the total volume of each island shape per unit surface area by summing over the island volumes in Figure 1b. (Note that the absolute value of the coverage determined by RBS and the island volume by AFM differ because of the presence of an ~ 3 eq-ML wetting layer and the fact that tip broadening and the surface oxide has an effect on the AFM measurements).

Figure 2 shows the integrated volume in each island shape as a function of the total amount of Ge in islands obtained from the preparation and AFM analysis of 35 different samples. For most of the samples, over 10 000 islands were measured and

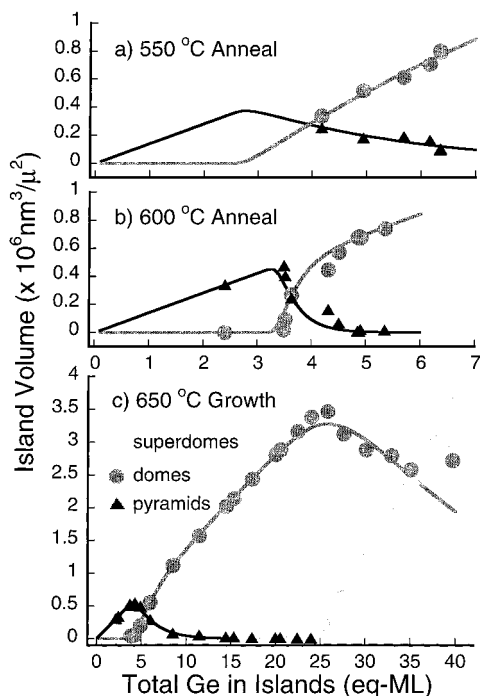


Figure 2. Integrated island volume (from AFM topographs) for each island shape as a function of the total amount of Ge in islands on Si-(001) for (a) 8 eq-ML of Ge annealed for various times at 550 °C, (b) 6 ML of Ge annealed for various times at 600 °C, and (c) increasing amounts of Ge deposited at 650 °C without annealing (pyramids, triangles; domes, circles; superdomes, diamonds). Each effective coverage corresponds to a separate sample, and the set of three figures represents statistics accumulated for about 500 000 islands. The solid lines represent fits of the data to the equilibrium model including interisland repulsions, eqs 1 and 4.

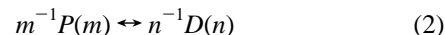
classified. Figure 2a,b involved the deposition of a fixed amount of Ge (8 and 6 eq-ML, determined by RBS) followed by annealing (at 550 and 600 °C, respectively) for various times. The size distributions of the islands evolved during the annealing process before eventually reaching a stable configuration. We concluded that Ge was moving from the wetting layer into the islands, and thus the islands were still growing after the deposition stopped.^{12,13} In Figure 2c, we show how the integrated island volumes evolve for a series of sequential depositions at 650 °C. The results of these and several other experiments can be summarized as follows: for small amounts of deposited Ge, only pyramids are present, and the integrated volume of pyramids increases linearly with amount of Ge deposited once the wetting layer thickness has been exceeded; after the first appearance of domes, the amount of Ge stored in pyramids decreases with an apparent exponential decay and eventually becomes a small fraction of the total Ge found in islands. The same type of transition is observed at higher coverages as domes give way to superdomes. This behavior during island growth is the similar to that observed in the real-time TEM observations of Ross et al.,¹⁶ who attributed the disappearance of smaller islands to Ostwald ripening. A major issue that must be addressed by the equilibrium model developed below is how to explain the coarsening of the islands observed during growth of Ge on Si(001) in Figure 2 and by Ross et al.¹⁶

To state the conservation of mass constraint on the system, the total Ge atom density residing in pyramids and domes (for example) on the substrate is

$$\Theta\rho = m\Omega_P + n\Omega_D \quad (1)$$

where Θ is the number of eq-ML of Ge measured in islands by AFM, ρ is the number density of Ge atoms in a monolayer, Ω_P is the surface density of all pyramids, m is the average number of atoms in a pyramid, Ω_D is the surface density of all domes, and n is the average number of atoms in a dome. The total integrated volume of Ge per unit surface area contained in pyramids is $V_P = om\Omega_P$ and in domes is $V_D = on\Omega_D$, where s is the volume of a single Ge atom.

Considered as a balanced chemical reaction, the pyramid to dome transition can be written



where $P(m)$ is an average volume pyramid and $D(n)$ is an average volume dome, to balance the reaction in terms of a single atom, which is possible because both the reactant and product contain only Ge. For noninteracting islands (an “ideal solution”), we have the following expression for the change in the free energy ΔF_{PD} for the reaction in eq 2

$$\Delta F_{PD} = n^{-1}F_D - m^{-1}F_P = \Delta F_{PD}^0 + k_B T \ln[\Omega_D^{1/n}/\Omega_P^{1/m}] \quad (3)$$

where F_P and F_D are the free energies of an average-sized pyramid and dome, respectively, ΔF_{PD}^0 is the standard free energy difference *per atom* between isolated pyramids and domes, k_B is the Boltzmann constant, and T is the temperature. If the system is at equilibrium, then $\Delta F_{PD} = 0$ and we have the usual relation between the standard free energy change for the reaction in eq 2 and the configurational entropy of the ideal island mixture, in this case expressed for convenience on a per atom basis.

Equation 3 can be solved subject to the constraints of equilibrium and conservation of mass to determine the dependence of V_P and V_D on Θ . At low coverages, most of the Ge is contained in pyramids, as one would expect from simple entropy arguments in order to maximize the number of islands on the surface. As the Ge coverage increases, the relative amount of material taken up by domes increases more rapidly than in pyramids, in accord with Le Chatelier’s principle. However, both V_P and V_D increase monotonically with Θ in an ideal island model, which does not agree qualitatively with the observations of Ross et al.¹⁶ nor the data in Figure 2.

The islands have significant strain fields, which have been imaged using TEM,²⁴ propagating through the Si substrate that should cause islands to effectively repel one another. This interaction was anticipated by Shchukin et al.,¹⁸ who explicitly included an interisland repulsion term in their description of the free energy of the island ensembles. This factor was utilized in the determination of the coverage versus lattice-mismatch phase diagrams for heteroepitaxy derived by Daruka and Barabasi.¹⁹ In addition, Floro et al.²⁵ have invoked interisland repulsion to explain the shift they observed to lower characteristic volumes for the transition of pyramids to domes for Si_{0.8}-Ge_{0.2}/Si(001) as the island density increases. Instead of replacing the island area densities by activities in eq 3, we will heuristically account for the nonideality of the island ensembles by subtracting an interisland repulsion term averaged over all island interactions, $\epsilon_{PD}\Theta$, from the standard free energy difference to obtain

$$\Omega_D^{1/n}/\Omega_P^{1/m} = \exp[-(\Delta F_{PD}^0 - \epsilon_{PD}\Theta)/k_B T] \quad (4)$$

This Θ dependence causes the equilibrium to shift more strongly in favor of the domes with increasing material deposition because domes contain more atoms per unit substrate surface

TABLE 1: Summary of Thermodynamic Data

	$\Delta E/k_B$	$\Delta S/k_B$	ϵ/k_B
pyramids to domes	$(0.198 \pm 0.050) \text{ K}$	$(4.44 \pm 4.0) \times 10^{-5}$	$(0.013 \pm 0.004) \text{ K/eq-ML}$
domes to superdomes	$(-0.0288 \pm 0.0090) \text{ K}$	$(-4.56 \pm 1.0) \times 10^{-5}$	$(4.62 \pm 3.0) \times 10^{-5} \text{ K/eq-ML}$

area, and thus store Ge more efficiently than pyramids. The choice of the appropriate exponent for Θ in eq 4 is not completely clear. Shchukin et al.¹⁸ assumed that the interisland repulsion was proportional to $\Theta^{3/2}$ on the basis of an analogy to repulsive dipole interactions, whereas our experimental results agreed better with Θ^1 . The solid lines shown in Figure 2 represent fits to the expression obtained on combining eqs 1 and 4, using ΔF_{PD}^0 and ϵ_{PD} as parameters for pyramid and dome populations and similarly derived parameters ΔF_{DS}^0 and ϵ_{DS} for dome and superdome populations. Thus, rather than being the result of Ostwald ripening, the disappearance of pyramids (domes) from a growing population of domes (superdomes) is completely consistent with an equilibrium system in which interisland repulsions squeeze out smaller islands as Ge is added because they store atoms less efficiently.

Examining the experimental results of many researchers^{4-7,13} shows that the relative populations of pyramids, domes, and superdomes on a surface is a complicated function of Ge coverage and temperature. We used our thermodynamic equations to construct the boundaries of a stability map (or shape diagram) for the islands. In order to construct such a map, it was necessary to determine the explicit temperature dependence of the standard free energy change of the islands in transforming from one shape to another²⁶

$$\Delta F_{PD}^0 = \Delta E_{PD}^0 - T\Delta S_{PD}^0 \quad (5)$$

where ΔE_{PD}^0 is the change in the standard internal energy (chemical and mechanical) of the island shapes and ΔS_{PD}^0 is the change in the standard internal entropy of the islands, which comes about by differences in the phonon states in the islands, for example. This shows that the parameters in the Shchukin et al.¹⁸ expression for the size dependence of the island free energy are also functions of temperature. Substituting eq 5 into eq 4 provides an explicit functional relationship between the total Ge substrate coverage and the temperature of the system. If we choose a particular constraint, for example, that the total integrated volume contained in pyramids equals the total integrated volume in domes, $V_P(\Theta) = V_D(\Theta)$, then we can plot a contour for this equality on a Θ versus T diagram that separates the region for which most of the Ge resides in domes from those dominated by pyramids or superdomes. This plot shows the temperature dependence of the coverage at which the integrated volumes of two shapes intersect in Figure 2. Figure 3 shows the shape map that resulted from using experimental data¹³ at 550 and 600 °C along with eqs 1, 4, and 5 (data at 650 °C was not used because of the obvious alloying).

One of the most striking features of the shape diagram in Figure 3 is that the slope of the boundary between the pyramids and domes is negative while that separating the domes and superdomes is positive. Equation 5 shows that the slopes of these boundaries are related to the difference in internal energy ΔE^0 (not free energy) between island shapes. Thus, our experimental results qualitatively indicate that the pyramid-to-dome transition is endothermic but the dome-to-superdome transition is exothermic. The quantitative results from our data are shown in Table 1. The shape diagram of Figure 3 also shows that the population of domes should be extremely low at temperatures below 500 °C, since at that temperature the pyramid-dome boundary intersects the dome-superdome

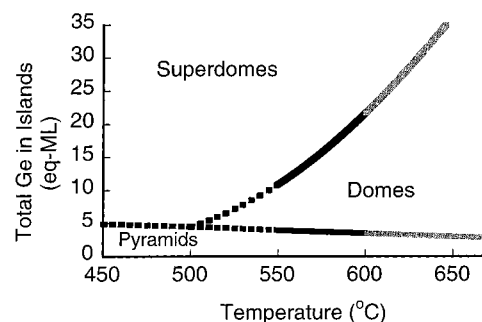


Figure 3. Shape diagram for Ge nanocrystals on Si(001) determined from experimental data on annealed samples at 8 and 13 eq-ML coverage at 550 °C and 6 and 11 eq-ML coverage at 600 °C. The horizontal axis represents the temperature at which the equilibrium of the island distribution is achieved, and the vertical axis is the amount of Ge in islands expressed in eq-ML. Since the AFM is not sensitive to the Ge in the wetting layer, this portion of the deposited Ge is not included on the diagram. The wetting layer is estimated to be between 1 and 3 eq-ML and may be temperature dependent. The map is divided into three primary regions, those in which most of the Ge resides in pyramids, domes, and superdomes. The boundaries represent the conditions for which two different shapes contain equal amounts of Ge. Any of the three shapes can be found in any of the regions at equilibrium, but the relative amounts of Ge in each shape can vary by many orders of magnitude, making it extremely unlikely to find certain shapes in some regions of the map.

boundary. Thus, the equilibrium shape diagram predicts that domes cannot be the majority species on Si(001) for temperatures less than 500 °C; they are adventitious structures that can appear because they store more atoms per unit substrate surface area than pyramids.

A stability map such as Figure 3 is valuable primarily if it can predict results not used in its construction. In fact, the shape diagram derived from our experimental data at 550 and 600 °C and extrapolated to lower temperatures resolves the anomalous behavior noted above with regard to the experimental results of Eaglesham and Cerullo² and Mo et al.³ Considering the experimental uncertainties in their different methods of measuring sample temperatures and overlayer coverages, the two groups were probably exploring different regions of the shape diagram in Figure 3. Mo et al.³ were most likely working at a lower absolute temperature, where the probability of finding domes is very low, than were Eaglesham and Cerullo.² By chance, both groups chose the temperature near which the behavior of the Ge on Si(001) system changes most significantly, and thus they obtained radically different results.

Given the small data set used to generate the shape diagram and the experimental uncertainties of different groups, the map in Figure 3 is in reasonable agreement with the experimental observations of many researchers (only a few of which will be mentioned here). Krishnamurthy et al.⁵ pointed out explicitly that their Ge overlayers deposited on 375 °C Si(001) substrates were dominated by very small islands at coverages at and below 7 eq-ML and very large islands (obviously superdomes from their scanning electron microscope images) for 9 eq-ML, with the transition between the two regimes appearing to be quite abrupt. In extensive experiments, Goldfarb et al.²⁷ have never observed domes on samples grown at substrate temperatures below 500 °C, but they have observed much larger structures that may be ill-formed superdomes. The fact that Tomitori et

al.⁴ observed the first appearance of superdomes but no domes on a 6 eq-ML sample grown at 400 °C and the first appearance of domes but no superdomes on a 7 ML sample grown at 500 °C is also in striking agreement with the shape map. At temperatures ≥ 650 °C, experimental data are not expected to agree with the shape map of Figure 3, which is calculated for pure Ge overlayers. Alloying with Si decreases the strain energy of the islands and thus shifts the boundaries between shapes to larger values of Θ for a particular temperature.

We have modeled strained epitaxial Ge nanocrystals on Si-(001) as giant adsorbed molecules or n -mers and have examined how equilibrium and mass conservation constraints can be applied to understand the shape evolution of the islands during growth. By including with the island standard free energy an interisland repulsion term proportional to the total Ge contained in islands θ , we have analyzed the growth behavior of the islands for which pyramids first grow and then disappear as domes grow; this behavior has been cited previously as strong evidence for Ostwald ripening.¹⁶ Finally, a chemical-thermodynamic treatment permits the construction of a shape diagram for the temperature and coverage behavior of pyramids, domes, and superdomes (assuming superdomes are also equilibrium structures, which appears to be the case from our annealing experiments). This map agrees with data collected on annealed island shape populations in this laboratory at 550 and 600 °C by construction, but it was also found to be consistent with the observations of several other researchers at significantly lower temperatures. Since nanocrystals are often regarded as transitional structures between molecules and bulk materials, the present molecular model represents one limiting case with the other being a macroscopic phase diagram;²⁸ the actual behavior of the Ge islands is expected to interpolate between these two extremes.

Acknowledgment. We thank A.-L. Barabasi, A. Bratkovski, G. A. D. Briggs, I. Goldfarb, and H. Reiss for many stimulating conversations and significant assistance during the course of this research.

References and Notes

- (1) Bauer, E. Z. *Kristallogr.* **1958**, *110*, 372.
- (2) Eaglesham, D. J.; Cerullo, M. *Phys. Rev. Lett.* **1990**, *64*, 1943.
- (3) Mo, Y.-W.; Savage, D. E.; Swartzentruber, B. S.; Lagally, M. G. *Phys. Rev. Lett.* **1990**, *65*, 1020.
- (4) Tomitori, M.; Watanabe, K.; Kobayashi, M.; Nishikawa, O. *Appl. Surf. Sci.* **1994**, *76/77*, 322.
- (5) Krishnamurthy, M.; Drucker, J. S.; Venables, J. A. *J. Appl. Phys.* **1991**, *69*, 6461.
- (6) Sakai, A.; Tatsumi, T. *Phys. Rev. Lett.* **1993**, *71*, 4007; *Appl. Phys. Lett.* **1994**, *64*, 52.
- (7) Eaglesham, D. J.; Hull, R. *Mater. Sci. Eng. B* **1995**, *30*, 197.
- (8) Hammar, M.; LeGoues, F. K.; Tersoff, J.; Reuter, M. C.; Tromp, R. M. *Surf. Sci.* **1996**, *349*, 129.
- (9) Kamins, T. I.; Carr, E. C.; Williams, R. S.; Rosner, S. J. *J. Appl. Phys.* **1997**, *81*, 211.
- (10) Medeiros-Ribeiro, G.; Bratkovski, A. M.; Kamins, T. I.; Ohlberg, D. A. A.; Williams, R. S. *Science* **1998**, *279*, 353.
- (11) Kamins, T. I.; Medeiros-Ribeiro, G.; Ohlberg, D. A. A.; Williams, R. S. *Appl. Phys. A*, in press.
- (12) Medeiros-Ribeiro, G.; Kamins, T. I.; Ohlberg, D. A. A.; Williams, R. S. *Phys. Rev. B* **1998**, *58*, 3533.
- (13) Kamins, T. I.; Medeiros-Ribeiro, G.; Ohlberg, D. A. A.; Williams, R. S. *J. Appl. Phys.*, in press.
- (14) Dorsch, W.; Strunk, H. P.; Wawra, H.; Wagner, G.; Groenen, J.; Carles, R. *Appl. Phys. Lett.* **1998**, *72*, 179.
- (15) Tersoff, J.; LeGoues, F. K. *Phys. Rev. Lett.* **1994**, *72*, 3570.
- (16) Ross, F. M.; Tersoff, J.; Tromp, R. M. *Phys. Rev. Lett.* **1998**, *80*, 984.
- (17) Zinke-Allmang, M.; Feldman, L. C.; Grabow, M. H. *Surf. Sci. Rep.* **1992**, *16*, 381.
- (18) Shchukin, V. A.; Ledentsov, N. N.; Kop'ev, P. S.; Bimberg, D. *Phys. Rev. Lett.* **1995**, *75*, 2968.
- (19) Daruka, I.; Barabasi, A.-L. *Phys. Rev. Lett.* **1997**, *79*, 3708; *Appl. Phys. Lett.* **1998**, *72*, 2102.
- (20) Steinfert, A. J.; Scholte, P. M. L. O.; Ettema, A.; Tuinstra, F.; Nielsen, M.; Landemark, E.; Smilgies, D.-M.; Feidenhans'l, R. *Phys. Rev. Lett.* **1996**, *77*, 2009.
- (21) Christiansen, S.; Albrecht, M.; Strunk, H. P.; Hansson, P. O.; Bauser, E. *Appl. Phys. Lett.* **1995**, *66*, 574.
- (22) Johnson, H. T.; Freund, L. B. *J. Appl. Phys.* **1997**, *81*, 6081.
- (23) Yu, W.; Madhukar, A. *Phys. Rev. Lett.* **1997**, *79*, 905. See also the erratum: *Phys. Rev. Lett.* **1997**, *79*, 4939.
- (24) Kolosov, O.; Castell, M.; Marsh, C.; Briggs, G. A. D.; Kamins, T. I.; Williams, R. S. *Phys. Rev. Lett.* **1998**, *81*, 1046.
- (25) Floro, J. A.; Lucadamo, G. A.; Chason, E.; Freund, L. B.; Sinclair, M.; Twisten, R. D.; Hwang, R. Q. *Phys. Rev. Lett.*, in press.
- (26) Lewis, G. N.; Randall, M. *Thermodynamics*; Revised by Pitzer, K. S.; Brewer, L.; McGraw-Hill: New York, 1961; pp 242-280.
- (27) Goldfarb, I.; Hayden, P. T.; Owen, J. H. G.; Briggs, G. A. D. *Phys. Rev. B* **1997**, *56*, 10459.
- (28) Briggs, G. A. D.; Sutton, A. P. Unpublished private communication.